ment. We therefore expect ^{17}O NMR to play an important role in the better understanding of oxidation processes where the source of oxygen is hydrogen peroxide or alkyl hydroperoxides.

Evidence against an Exchange of Oxygen between Oxo and Peroxo Groups in Mo(VI) Derivatives. Peroxo species appear to play a determinant role in vanadium(V)- or molybdenum(VI)-catalyzed oxidations by hydrogen peroxide;[21] however, the structure of the peroxo moiety, i.e., identification of the actual oxidizing species, is still uncertain. Modena et al. recently proposed that, in the presence of water, one of the following exchange reactions takes place:[13]

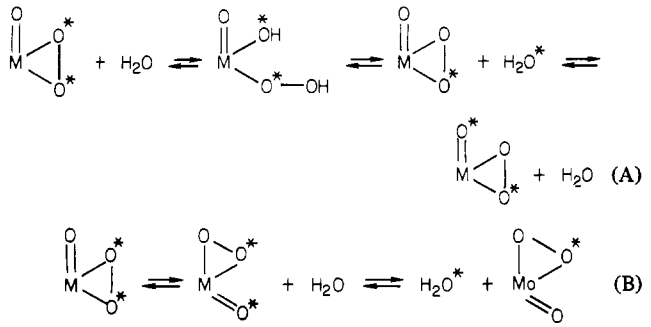

(A)

(B)

If one of these exchanges were taking place, it would result for compound **1** in a random scrambling of the labeled oxygen atoms between $H_2{}^{17}O$ and the Mo=O and

groups: the areas of the two ^{17}O signals for **1** would then be in a 1/2 ratio and not 1/6 as we measured (Figure 2b).

Definite evidence against the occurrence of the oxo-peroxo exchange was obtained by comparing the ^{17}O NMR spectra of **1** measured in CH_2Cl_2 solutions (8×10^{-2} M) to which a tenfold amount (8×10^{-1} M) of either $H_2{}^{16}O$ or $H_2{}^{17}O$ (10%) was added. After 1 h, only one signal was detected in the ^{17}O NMR of the $H_2{}^{16}O$-containing sample, which corresponded to the peroxo group, instead of the two signals observed when $H_2{}^{17}O$ was present (vide supra). Taking into account the fact that the line width of the (^{17}O)peroxo signal is ca. 20 times wider than that of a terminal oxo group, the nondetection of a Mo=^{17}O signal means that the rate of exchange, if any, is too slow to be of any significance in a catalytic process.

Conversely when we measured the ^{17}O NMR spectra for the series of MoO_5·L compounds listed in Table I after addition of 10% ^{17}O-enriched water, i.e., after labeling of the oxo group specifically, we could not detect any peroxo signal, even after a 48 h contact with $H_2{}^{17}O$.

We interpret these results to mean that intra- or intermolecular oxygen exchange between the oxo and the peroxo groups in these Mo(VI) oxo peroxo derivatives does not take place to a measurable extent, and therefore is unlikely to be involved as a key step in Mo(VI)-catalyzed oxidations by hydrogen peroxide.

In conclusion, peroxidic oxygen atoms can be observed through ^{17}O NMR on Mo(VI) and Pt(II) compounds. Not only structural but also mechanistic information can be gained through this spectroscopy. As an example the absence of significant detectable oxo vs. peroxo oxygen exchange in Mo(VI) derivatives was established.

Our results clearly indicate that ^{17}O NMR should be an efficient tool in the study of peroxidic transition-metal derivatives provided there is no exchange with molecular dioxygen. However, ^{17}O-enriched samples will generally be necessary in order to record the ^{17}O spectra in reasonable conditions.

Acknowledgment. We are grateful to Dr. H. Mimoun of the Institut Français du Pêtrole, for a gift of the platinum alkyl peroxide compound, and to Dr. F. Casabianca of the Nice Laboratory for his contribution in synthesizing the molybdenum oxo diperoxo complexes. Acknowledgment is made to the donors of the Petroleum Research Fund, administered by the American Chemical Society, for partial support of this work.

Registry No. 1, 82281-65-0; **2**, 79359-93-6; $MoO(O_2)_2$·HMPA, 25377-12-2; $MoO(O_2)_2$·py, 67228-13-1; $MoO(O_2)_2$·picH, 67584-06-9; $MoO(O_2)$dipic, 69594-30-5; $MoO(O_2)_2$·DMLA (R = H; R^1 = Me), 70355-53-2; $MoO(O_2)_2$·DMLA (R = Me, R^1 = Me), 85735-46-2; $MoO(O_2)_2$·DMCOLA (R = H; R^1 = COPh), 85748-26-1; ^{17}O, 13968-48-4.

(21) Sheldon, R. A. "Aspects of Homogeneous Catalysts"; Ugo, R., Ed.; D. Reidel: London, 1981, Vol. IV.

EPR Evidence on the Structure of the Copper(II)-Bacitracin A Complex

Edmund G. Seebauer, Edward P. Duliba, Duane A. Scogin, Robert B. Gennis, and R. L. Belford*

Contribution from the School of Chemical Sciences, University of Illinois, Urbana, Illinois 61801. *Received October 12, 1982*

Abstract: Bacitracin is an antibiotic that is effective only in the presence of divalent metal cations. In this paper, the possible sites for the binding of divalent transition metal ions to bacitracin A are investigated by electron paramagnetic resonance. Manganese(II) shows only the characteristics of the aqueous ion. High-spin cobalt, suggesting distorted octahedral coordination, is indicated from the cobalt(II) EPR spectra. The copper(II) complex yields a rich spectrum and detailed structural information. The electronic Zeeman, hyperfine, and nuclear quadrupole coupling parameters show that copper is most probably square planar, coordinated to the glutamate γ-carboxyl, the histidine imidazole, the aspartate β-carboxyl, and the thiazoline nitrogen. This is the first reported case of a significant influence of quadrupole coupling on the EPR spectra of solutions of metal compounds of such complexity or of biological significance.

Bacitracin A (see Figure 1) is the major component of a group of closely related polypeptide antibiotics produced by *Bacillus licheniformis*. Bacitracin A is a dodecapeptide that acts against Gram-positive bacteria, apparently by blocking a critical step in cell wall synthesis.[1] This step is the dephosphorylation of the lipid carrier intermediate C_{55}-bactoprenyl pyrophosphate.[2] Strominger et al. have shown that bacitracin A forms a stoi-

(1) Robinson, F. A. "Antibiotics"; Pitman and Sons, Ltd.: London, 1953, pp 107-111.

0002-7863/83/1505-4926$01.50/0

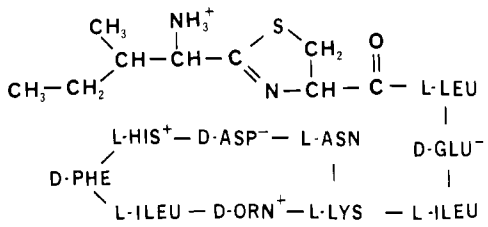

Figure 1. Structure of bacitracin A. The charges shown are for the molecule at neutral pH.[13]

chiometric 1:1 complex with long-chain polyisoprenyl pyrophosphates.[3,4] The complex is strong but requires the presence of a divalent metal cation such as Zn^{2+}. Adler et al. presented evidence that the antibiotic activity of bacitracin results from such a complex.[5] The bacitracin is ineffective in the absence of divalent metal cations. Furthermore, the number of bacitracin molecules bound to *Micrococcus lysodeikticus* cells has been shown to be roughly equal to the number of bactoprenyl pyrophosphate molecules present.[6]

The metal binding properties of bacitracin A are of significant interest because such systems may provide a general model for the activation of enzymes by metal ions. Although bacitracin A has been shown to bind to divalent cations such as copper, nickel, zinc, cobalt, and manganese, the structure of the complex has been the source of considerable debate for two decades.[7-10] Suggestions have been made that metal ions coordinate to (1) the thiazoline ring, (2) the histidine imidazole, (3) the terminal isoleucine amino group, (4) the histidine peptide nitrogen, and (5) both carboxyl groups. However, all workers agree that the ornithine amino group does not participate directly in metal coordination.

Bacitracin A has been studied by a wide variety of methods including proton release titration,[7,11] optical rotatory dispersion spectroscopy,[8] ultraviolet absorption spectroscopy,[8,11] pH titration,[7,12] circular dichroism spectroscopy,[11] chemical protection experiments with fluoro-2,4-dinitrobenzene[8] and 2,4,6-trinitrobenzenesulfonate,[13] ^1H NMR,[9,14,15] ^{13}C NMR,[10] tritium exchange,[16] and dark-field electron microscopy combined with optical filtering.[17]

The purpose of this study is to clarify the nature of the divalent metal ion coordination to bacitracin A by employing a different experimental technique: electron paramagnetic resonance (EPR). The utilization of computer simulation of powder-type EPR spectra has proven effective for the elucidation of molecular information.[18,19] Electric quadrupole coupling effects on the EPR spectrum from quadrupolar copper nuclei were previously shown to be useful for the determination of local site geometry.[19,20] In particular, the larger quadrupole coupling parameters are associated with increased environmental symmetry.

The results of EPR studies of the frozen aqueous solutions and magnetically dilute polycrystalline powders of bacitracin A with several paramagnetic transition metal ions will be presented. Conclusions based upon the computer simulation and interpretation of the quadrupole coupling parameters will be drawn about the structures of these complexes, particularly concerning the complex with divalent copper.

Experimental Section

Commercial bacitracin, which is a mixture of several similar peptides, was donated by the IMC Chemical Group, Terre Haute, IN. Bacitracin A was isolated from the mixture by countercurrent distribution, and inorganic phosphate removed by anion-exchange chromatography by the method of Scogin.[11,13] Ultraviolet absorption spectroscopy at 292 nm showed the bacitracin A to be free of its decomposition product, bacitracin F. The yellowish white solid was stable when stored at −15 °C.

Aqueous solutions of bacitracin A with copper(II), cobalt(II), and manganese(II) were prepared from mixtures of aqueous solutions of bacitracin A and the metal chloride. The resulting solutions were adjusted to contain 25 vol % glycerin to ensure proper freezing characteristics. The samples were always 30 mM in bacitracin A but had metal ion concentrations ranging from 0.5 to 6.7 mM. Unbuffered samples prepared from copper or cobalt had a pH of 5.2. No buffer was used because a strong acetate buffer was found to distort and decrease the resolution of the EPR spectrum for copper. However at pH 5.2, the association constant of the manganese complex is too small to ensure complete metal complexation.[13] Therefore, the manganese samples were adjusted to pH 7.1 with NaOH to increase the association to an acceptable level. At this pH, a small amount of precipitate was observed.

Magnetically dilute polycrystalline samples of bacitracin A with the previous metals were made with the nickel(II)–bacitracin A complex as the diamagnetic host. The preparation procedure took advantage of the low solubility of these complexes at high pH. An aqueous solution of nickel(II) chloride and the desired paramagnetic ion was added to an aqueous 35 mM solution of bacitracin A whose pH had been adjusted to 7.5 with NaOH. The pH was kept low enough to prevent the oxidation of the N-terminal isoleucine and the thiazoline ring that occurs in excessively alkaline solutions. The metal ion solution contained sufficient nickel to complex 96% of the bacitracin A and approximately 1.5 times the amount of paramagnetic metal needed to react with the remaining 4%. Competition of the excess paramagnetic metal with nickel for binding sites was negligible because the association constant for the nickel complex is at least 60 times that of the other metals at the pH of interest.[13]

Reagent grade divalent chlorides of nickel, copper, cobalt, and manganese were used for all experiments. However, the cobalt(II) chloride was treated in an ion exchange column employing Dowex 1-X8 (20–50 mesh) resin, according to the method of Kraus and Moore,[21] to eliminate paramagnetic copper and manganese contamination. After recrystallization from an acetone–dichloromethane mixture, the product showed no paramagnetic contamination.

EPR spectra of all samples were recorded at 77 K on a Varian E-9 X-band (9.5 GHz) spectrometer. The temperature was maintained by a liquid-nitrogen-cooled nitrogen gas stream. Magnetic field strength was monitored with a Bruker B-NM20 tracking NMR oscillator. Frequencies were determined with a Hewlett-Packard 5240-A digital frequency meter.

Computer simulations used the program QPOW developed by Nilges and Belford.[18,22] For powder simulations, a four-point Gauss-point integration is used. The computer program allows consideration of the electronic g, hyperfine, isotropic nuclear g, nuclear quadrupole, and superhyperfine matrices and nonalignment of the principal axes of the hyperfine, superhyperfine, and quadrupole matrices with Euler angles according to the convention of Rose.[23] Calculations utilized the University of Illinois VAX/VMS-11 computer, and simulations were displayed on Houston Instruments digital plotters. The input parameters

(2) Siewert, G.; Strominger, J. L. *Proc. Natl. Acad. Sci. U.S.A.* **1967**, *57*, 767–773.
(3) Stone, K. J.; Strominger, J. L. *Proc. Natl. Acad. Sci. U.S.A.* **1971**, *68*, 3223–3227.
(4) Storm, D. R.; Strominger, J. L. *J. Biol. Chem.* **1973**, *248*, 3940–3945.
(5) Adler, R. H.; Snoke, J. E. *J. Bacteriol.* **1962**, *83*, 1315–1317.
(6) Storm, D. R.; Strominger, J. L. *J. Biol. Chem.* **1974**, *249*, 1823–1827.
(7) Garbutt, J. T.; Morehouse, A. L.; Hanson, A. M. *J. Agric. Food Chem.* **1961**, *9*, 285.
(8) Craig, L. C.; Phillips, W. F.; Burachik, M. *Biochemistry* **1969**, *8*, 2348–2356.
(9) Cornell, N. W.; Guiney, D. G., Jr. *Biochem. Biophys. Res. Commun.* **1970**, *40*, 530–536.
(10) Wasylishen, R. E.; Graham, M. R. *Can. J. Biochem.* **1975**, *53*, 1250–1254.
(11) Scogin, D. A.; Mosberg, H. I.; Storm, D. R.; Gennis, R. B. *Biochemistry* **1980**, *19*, 3348–3352.
(12) Bradshaw, R. A.; Shearer, W. T.; Gurd, F. R. N. *J. Biol. Chem.* **1968**, *243*, 3817–3825.
(13) Scogin, D. A. Ph.D. Thesis, University of Illinois, Urbana, IL, **1981**.
(14) Campbell, I. D.; Dobson, C. M.; Jeminet, G.; Williams, R. J. P. *FEBS Lett.* **1974**, *4*, 115.
(15) Mosberg, H. I.; Scogin, D. A.; Storm, D. R.; Gennis, R. B. *Biochemistry* **1980**, *19*, 3353–3357.
(16) Galardy, R. E.; Printz, M. P.; Craig, L. C. *Biochemistry* **1979**, *10*, 2429–2436.
(17) Ottensmeyer, F. P.; Bazett-Jones, D. P.; Hewitt, J.; Price, G. B. *Ultramicroscopy* **1978**, *3*, 303–313.
(18) Belford, R. L.; Nilges, M. J. Symposium on Electron Paramagnetic Resonance Spectroscopy, Rocky Mountain Conference on Analytical Chemistry, Denver, CO, Aug 1979, Paper No. 59, in press.
(19) Duan, D. C.; Belford, R. L. *J. Magn. Reson.* **1978**, *29*, 293–307.
(20) So, H.; Belford, R. L. *J. Am. Chem. Soc.* **1969**, *91*, 2392–2394.
(21) Kraus, K. A.; Moore, G. E. *J. Am. Chem. Soc.* **1953**, *75*, 1460–1462.
(22) Nilges, M. J. Ph.D. Thesis, University of Illinois, Urbana, IL, 1979.
(23) Rose, M. E. "Elementary Theory of Angular Momentum"; Wiley: New York, 1957; pp 50–51.

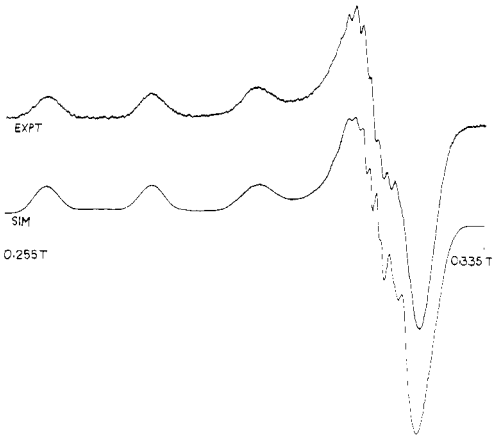

Figure 2. Best fit between the experimental and simulated EPR spectra of copper(II)–bacitracin A frozen solution. Instrument parameters: ν = 9.11207 GHz, 80-mT scan range centered at 295.0 mT, time constant = 1.0 s, 16-min scan, 0.08-mT peak-to-peak modulation at 100 kHz, microwave power = 3.0 mW, receiver gain = 5000, temperature = 77 K. Simulation parameters: ν = 9.11207 GHz, g_x = 2.0575, g_y = 2.0469, g_z = 2.2610, A_x = −60.0 MHz, A_y = −53.4 MHz, A_z = −543.6 MHz, $\alpha = \gamma = 0.0°$, $\beta = 3.0°$, B_x = 37.5 MHz, $B_y = B_z$ = 31.5 MHz, QD = 16.0 MHz, QE = 0.0 MHz, Gaussian linewidths of 17, 17, and 36 MHz for the x, y, and z components, respectively, and g_n = 1.4820.[31]

are varied until a good visual fit is obtained between the experimental and simulated spectrum. The simulated spectra were based on the following spin Hamiltonian:

$$\mathcal{H} = \beta H \cdot g \cdot S + \beta_n g_n H \cdot S + hS \cdot A \cdot I + hQD[I_z^2 - I(I+1)/3] + hQE(I_x^2 - I_y^2) + h\sum_{i=1}^{2} S \cdot B \cdot I_i$$

Results

Manganese. The spectrum of the frozen manganese–bacitracin A solution revealed only the six-line absorption characteristic of aqueous manganese at concentrations of 0.5 and 1.0 mM. The spectrum of the polycrystalline manganese–bacitracin A sample showed no signal.

Cobalt. The cobalt–bacitracin A frozen solution exhibited no signal. The EPR spectrum of the magnetically dilute cobalt powder complex revealed a single, nearly featureless pattern extending from 0 to 0.270 T.

Copper. The copper–bacitracin a complex proved most amenable to EPR analysis. Samples were run with copper concentrations ranging from 0.7 to 6.7 mM, but a concentration of 4.5 mM gave the strongest signal without concentration broadening. The spectrum (see Figure 2) displays distinct but overlapping parallel and perpendicular regions at lower and higher magnetic fields, respectively. Each region is split into four main peaks due to the copper hyperfine interaction ($I = {}^3/_2$). The high-field parallel line is obscured by the perpendicular region. The perpendicular peaks are further split by superhyperfine interaction with two nitrogen nuclei (I = 1), producing the additional structure. The principal axes of the hyperfine matrix are noncollinear with the principal axes of the electronic Zeeman matrix, creating the large off-axis extremum at the high-field end of the spectrum.

The magnetically dilute copper powder revealed two distinct magnetic sites (see Figure 3). One site is exactly equivalent to that observed in the frozen solution. The second site differs significantly in the parallel region. Samples were dried under vacuum for 2 days to remove any residual water. However, the resulting spectrum was identical with the initial powder spectrum. The solid was dissolved in dilute HCl and reprecipitated by addition of 1 M NaOH. The EPR spectrum differed only in a slight increase in the intensity of the second site and some perpendicular line broadening.

Discussion

Manganese. Two explanations are possible for the manganese solution spectrum. Firstly, the manganese may be only weakly bound to bacitracin A. Secondly, the manganese may be more strongly bound but in an environment similar to that in solution. We cannot distinguish between these alternatives with our data. However, several other workers have found only weak interactions between manganese and bacitracin A. Garbutt et al.[7] found that manganese does not bind to bacitracin A below pH 7, and then only to the N-terminal isoleucine group. Scogin[13] could not saturate bacitracin A at pH 5 even with a large excess of manganese.

For the manganese-doped powder spectrum, it is probable that dipolar interactions between the manganese centers in the solid broadened the absorption lines until they were unobservable. Upon addition of the nickel–manganese solution to the bacitracin A, the pH dropped from 7.5 to 6.4, below that required for the manganese to precipitate. Although the pH was then adjusted back to 7.5, coprecipitation of the nickel and manganese complexes probably was not achieved.

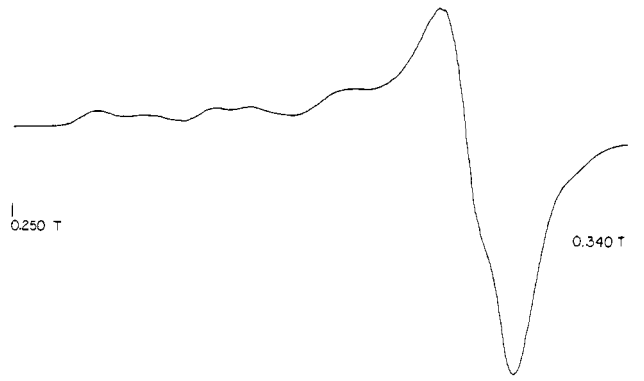

Figure 3. Experimental EPR spectrum of 4% copper-doped nickel–bacitracin A powder. Instrument parameters: ν = 9.11564 GHz, 90-mT scan range centered at 295.0 mT, time constant = 0.03 s, 4-min scan, 0.10 mT peak-to-peak modulation at 100 kHz, microwave power = 3.0 mW, receiver gain = 630, temperature = 77 K.

Table I. Copper(II)–Bacitracin A Frozen Solution EPR Parameters

Electronic Zeeman	Copper Hyperfine (10^{-4} cm^{-1})
g_x = 2.0575 ± 0.0003	A_x = −20.0 ± 0.2 (−60.0 MHz)
g_y = 2.0469 ± 0.0003	A_y = −17.8 ± 0.2 (−53.4 MHz)
g_z = 2.2610 ± 0.0003	A_z = −178.0 ± 0.2 (−534.0 MHz)
	$\alpha = \gamma = 0.0°$, $\beta = 3.0 \pm 0.2°$
Nitrogen Superhyperfine (10^{-4} cm^{-1})	Copper Quadrupole (10^{-4} cm^{-1})
B_x = 12.5 ± 0.2 (37.5 MHz)	QD = 5.3 ± 0.2 (15.9 MHz)
B_y = 10.5 ± 0.2 (31.5 MHz)	QE = 0.0 ± 0.2 (0.0 MHz)
B_z = 10.5 ± 0.2 (31.5 MHz)	$\alpha = \gamma = 0.0°$, $\beta = 3.0 \pm 0.2°$
$\alpha = \gamma = 0.0°$, $\beta = 3.0 \pm 0.2°$	

Cobalt. The absence of a cobalt solution signal implies that the cobalt is in a high-spin state ($S = {}^3/_2$). For high-spin cobalt in a weak crystal field, spin–orbit coupling between the low-lying levels causes the spin–lattice relaxation times to be short. The resulting EPR spectra are commonly extremely broad and can only be observed at liquid-helium temperatures.[24] From the cobalt-doped powder spectrum, high-spin cobalt is again suggested, since low-spin cobalt does not absorb at fields as low as a few hundredths tesla.

Copper. The electronic Zeeman and hyperfine matrices of the solution spectrum (see Table I) as determined by computer simulation were typical of copper in an environment that is square planar or nearly so. The spectrum was best simulated assuming coordination to two equivalent or nearly equivalent nitrogen atoms. The $g_\parallel$ and $A_\parallel$ values agree well with those proposed by Peisach et al.[25] as being usual for square-planar copper coordinated to two nitrogen and two oxygen atoms. Coordination to the sulfur in

(24) McGarvey, B. R. In "Transition Metal Chemistry"; Carlin, R. L., Ed.; Marcel Dekker: New York, 1966; Vol. III, pp 175–178.
(25) Peisach, J.; Blumberg, W. E. *Arch. Biochem. Biophys.* **1974**, *165*, 691–708.

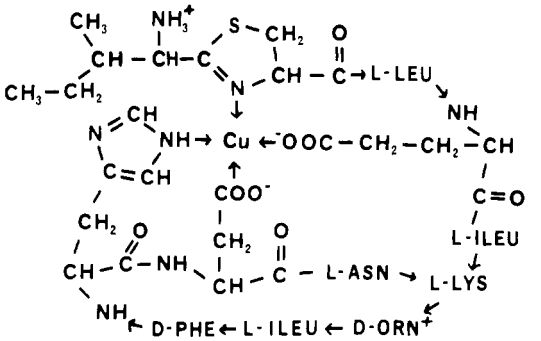

Figure 4. Proposed binding model for the copper(II)–bacitracin A complex.

the thiazoline ring is virtually ruled out because such coordination would greatly decrease both $g_{\parallel}$ and $A_{\parallel}$.

At least one conformation of bacitracin A exists where the copper is square planar: the copper is bonded to the glutamate γ-carboxyl, the histidine imidazole, the aspartate β-carboxyl, and the thiazoline nitrogen (see Figure 4). Such a structure is consistent with the possible extra bonding site proposed by Scogin[13] and the conclusion by Wasylishen et al.[10] that copper bonds to the aspartate carboxyl.

The observed anisotropy can result from several causes. Firstly, structurally inequivalent nitrogens can produce nonaxial parameters. However, Gould et al.[26] have demonstrated that in some copper–peptide systems, two structurally inequivalent nitrogen atoms can interact equivalently with the copper cation. Secondly, some anisotropy could be the product of the copper interacting with two different atoms: nitrogen and oxygen. Thirdly, axial coordination along the z-axis is possible, by water in the aqueous solution or by a nitrogen or carboxyl oxygen of the bacitracin A in the powder. The principal parameters can be relatively insensitive even to fairly strong x-axis coordination in an otherwise square-planar complex.[27,28]

This represents the first reported value of a nuclear quadrupole coupling parameter for copper(II) in a biological system. The sizable coupling is significant because it greatly improves the simulation and assists in defining the coordination symmetry. The quadrupole coupling parameter, 16.0 MHz, falls within the range characteristic of square-planar complexation with oxygen and nitrogen ligands, with either some out-of-plane coordination or some tetrahedral distortion.[19,29] Higher local site symmetry corresponds with larger quadrupole coupling values, with octahedral coordination giving a range of 30 to 33 MHz. The range for square-planar coordination is 9.6 to 13.5 MHz. With some out-of-plane coordination toward a tetragonal pyramid or tetrahedral distortion, the range increases to 15.9 to 18.6 MHz. Sulfur ligands tend to reduce quadrupole coupling of Cu(II) so severely that it is most unlikely that the Cu(II) in this bacitracin complex is coordinated to the sulfur of the thiazoline ring.[29]

The values of the second site measured from the copper-doped powder spectrum were $g_{\parallel} = 2.230 \pm 0.001$ and $A_{\parallel} = 459.0 \pm 0.5$ MHz. The perpendicular region was poorly resolved but not substantially shifted, and most of the observable fine structure retained its former position.

Sakaguchi et al.[30] have suggested the ratio $g_{\parallel}/A_{\parallel}$ as an empirical measure of the amount of tetrahedral distortion in copper complexes. They proposed a range of 105 to 135 cm for square-planar geometry. For $A_{\parallel}$ measured in cm^{-1}, the ratio is 126 cm for the solution complex and 146 cm for the second site in the powder. During crystallization, the complex may lose the fifth site coordination from water or another site on the bacitracin A molecule. Loss of this site may cause a more tetrahedral configuration to be favored. Complexation to water would seem to be ruled out, since careful drying failed to eliminate the first complex. Alternatively, if the fifth site is on the bacitracin, it would seem unlikely that the solution and solid complexes would differ so greatly.

A reasonable explanation is that the nickel host may form a tetrahedrally distorted complex and so attempt to force the copper dopant to assume a similar structure; some of the copper may exist as square-planar interstitial molecules or as defects in the crystal lattice. The concentration ratio of the two forms would be thermodynamically (equilibrium) or kinetically controlled during crystallization. This would explain the powder's insensitivity to drying and the constancy in the ratio of the two forms after reprecipitation.

Acknowledgment. This research was supported by grants from the National Science Foundation (Quantum Chemistry Program), National Institutes of Health (HL 16101), and by the University of Illinois and Arthur W. Sloan undergraduate research participation awards to E.G.S.

Registry No. Bacitracin A, 22601-59-8; copper(II), 15158-11-9; cobalt(II), 22541-53-3; manganese(II), 16397-91-4; copper–bacitracin A complex, 85800-09-5.

(26) Gould, D. C.; Mason, H. S. *Biochemistry* **1967**, *6*, 801–809.
(27) Addison, A. W.; Carpenter, M.; Lau, L. K. M.; Wicholas, M. *Inorg. Chem.* **1978**, *17*, 1545–1552.
(28) Freyburg, D. P.; Mockler, G. M.; Sinar, E. *Inorg. Chem.* **1977**, *16*, 1660–1665.
(29) (a) Liczwek, D. L.; Ph.D. Thesis, University of Illinois, Urbana, IL, 1982. (b) Liczwek, D. L.; Belford, R. L.; Pilbrow, J. R.; Hyde, J. S. *J. Phys. Chem.* **1983**, *87*, in press.
(30) Sakaguchi, U.; Addison, A. W. *J. Chem. Soc., Dalton Trans.* **1979**, 600–608.
(31) Fuller, G. H.; Cohen, V. W. *Nucl. Data, Sect. A5*, **1969**, 446.